

# Shoreline change assessment using multi-temporal satellite images: a case study of Lake Sapanca, NW Turkey

Umit Duru 

Received: 23 December 2016 / Accepted: 28 June 2017 / Published online: 7 July 2017  
© Springer International Publishing AG 2017

**Abstract** The research summarized here determines historical shoreline changes along Lake Sapanca by using Remote Sensing (RS) and Geographical Information Systems (GIS). Six multi-temporal satellite images of Landsat Multispectral Scanner (L1-5 MMS), Enhanced Thematic Mapper Plus (L7 ETM+), and Operational Land Imager Sensors (L8 OLI), covering the period between 17 June 1975 and 15 July 2016, were used to monitor shoreline positions and estimate change rates along the coastal zone. After pre-processing routines, the Normalized Difference Water Index (NDWI), Modified Normalized Difference Water Index (MNDWI), and supervised classification techniques were utilized to extract six different shorelines. Digital Shoreline Analysis System (DSAS), a toolbox that enables transect-based computations of shoreline displacement, was used to compute historical shoreline change rates. The average rate of shoreline change for the entire coast was 2.7 m/year of progradation with an uncertainty of 0.2 m/year. While the great part of the lake shoreline remained stable, the study concluded that the easterly and westerly coasts and deltaic coasts are more vulnerable to shoreline displacements over the last four decades. The study also reveals that anthropogenic activities, more specifically over extraction of freshwater from the lake, cyclic variation in rainfall, and deposition of sediment transported by the surrounding creeks dominantly control spatiotemporal

shoreline changes in the region. Monitoring shoreline changes using multi-temporal satellite images is a significant component for the coastal decision-making and management.

**Keywords** Landsat imagery · Shoreline change detection · DSAS · Coastal management · Lake Sapanca

## Introduction

Shoreline is defined as a contact line where land and water meet; shoreline position and its rate of change constitute fundamental knowledge for monitoring and management purposes. The change of shoreline is a naturally dynamic phenomenon, controlled by beach form, sediment characteristics, climate change, and anthropogenic effect. Rapid shoreline changes cause socioeconomic impacts (Bin et al. 2008; Paterson et al. 2010; Boahen et al. 2014), environmental consequences in aquatic ecosystems (Schindler and Scheuerell 2002; Lewin et al. 2014), and deteriorations of coastal ecosystems (Coops et al. 2003; Moussa et al. 2005), as well as geomorphic responses (Jangir et al. 2016; Kumari et al. 2012; Tonisso et al. 2012; Sudha Rani et al. 2015; Mann et al. 2016). The detection of shoreline change is a significant component for providing spatiotemporal analysis of freshwater resources. Therefore, numerous approaches have been applied to monitor and detect historical shoreline changes: Traditional field methods require a significant amount of labor, time, and cost, but it procures higher accuracy (Liu et al. 2007; Natesan

---

U. Duru (✉)  
Department of Geography, Sakarya University, 54187 Sakarya,  
Turkey  
e-mail: umitduru81@gmail.com

et al. 2013); monitoring historical shoreline changes using Remote Sensing (RS) and Geographical Information Systems (GIS) techniques has become increasingly important in the past decades because remotely sensed images provide historical snapshot of shoreline displacements utilizing digital imageries.

A reliable monitoring of temporal fluctuation in the volume of water within a lake does not only enable to track historical changes among time intervals (Wallick et al. 2006) but also makes it possible to work on larger areas more accurately and efficiently (Martin et al. 2005; Durduran 2010). In respect to various techniques in the field of shoreline displacements using RS and GIS, composing of the modern light detection and ranging (LIDAR) technique (Stockdon et al. 2002; Liu et al. 2007), the airborne laser scanner method (Zhang et al. 2005), video-based technology (Yoon et al. 2008; Bumshick and Kyuhan 2015), and synthetic aperture radar (SAR) imagery (Wang and Allen 2008; Al Fugura et al. 2011) provide more accurate statistics than satellite images, but the majority of these techniques are usually restricted due to the high cost of data acquisitions. Aerial and multispectral satellite imagery facilitate feasible and efficient tools for monitoring dynamic of the shorelines, cost-effectively (Kuleli 2010; Al-Hatrushi 2013), by comparing multi-temporal images. Hence, reliable monitoring of historical shoreline changes over larger areas may also provide better understanding of controlling factors on water level fluctuations at a regional scale. Numerous studies have been applying aerial photograph and multispectral satellite imagery to detect historical shoreline changes (e.g., Sener et al. 2009; El-Asmar and Hereher 2011; Ford 2013; Mujabar and Chandrasekar 2013).

Over the past decades, various studies have been done in the field of freshwater resources particularly lakes utilizing Landsat imageries. For instance, Tao et al. (2015) extensively investigated multi-temporal Landsat images between the late 1980 and 2000 in the Mongolian Plateau, and reported rapid loss of the lakes resulting from variation in precipitation, mining, and agricultural practices. However, so far, only a few studies have investigated historical shoreline changes in Turkey's lakes, for instance, Salt Lake (Ormeçi and Ekercin, 2007), Lake Uluabat (Tagil 2007), Lake Egirdir (Kalkan et al. 2013), Lake Acigol (Temiz and Durduran 2016), and Lake Burdur (Sarp and Ozcelik 2016). Overall conclusions from these studies indicate the lakes were experienced toward drying up based upon natural

and anthropogenic influences. A study was done using Landsat imageries on the shoreline in the basin of Lake Terkos (Bayram et al. 2013). According to this study, the main factor controlling historical shoreline changes in the region is related to uncontrolled human activities consisting of population growth, accordingly increasing demand for freshwater supply. Sener et al. (2009) have also observed changes in surface water area of Lake Akşehir and Eber from Landsat data, and they concluded that a rapid decrease of water level and area are mainly resulted from climate change.

Previous works (e.g., Kuleli 2010; Mujabar and Chandrasekar 2013; Nandi et al. 2016) mainly engaged manual digitization method to monitor only shoreline variation over time. However, the presented paper assessed the impacts of potential factors (e.g., climate and hydrology) on shoreline change, as well as testing the applicability of shoreline delineation using supervised classification, NDWI (Normalized Difference Water Index) and WNDWI (Modified Difference Water Index). Then, the classification method with the best statistical result was performed to extract shorelines and analyzed historical shoreline changes in an automated shoreline analysis interface in the region. The aim of this study is to develop a systematic methodology of monitoring historical shoreline displacements of Lake Sapanca using multi-temporal satellite processing techniques and to determine natural and anthropogenic influences on shoreline displacements. Finally, environmental impacts of shoreline displacement were also assessed within the studied region.

## Study area

Lake Sapanca is located 20 km east of the Gulf Izmit in the northwestern part of Turkey (Fig. 1). The drainage pattern along the study area is controlled by rainfall events, groundwater, and 18 flashy creeks, meaning that the water level is quick to rise and quick to fall. These creeks (Keci, Istanbul, Kurtkoy, Mahmudiye, Yanik, Karacay, Balikhane, Ciftecinar, Tuzla, Kuru, Esme, Cataloldu, Altikurus, Harmanlar, Aygır, Cehennem, Arifiye, Sarp) are mainly ephemeral, discharge varies seasonally, with higher flow in the winter and spring and lower flows during summer and early fall. The mean annual precipitation in Sapanca is 780 mm; the most of the precipitation falls during winter (32.6%); the lowest precipitation rate is seen in the summer (19.7%).

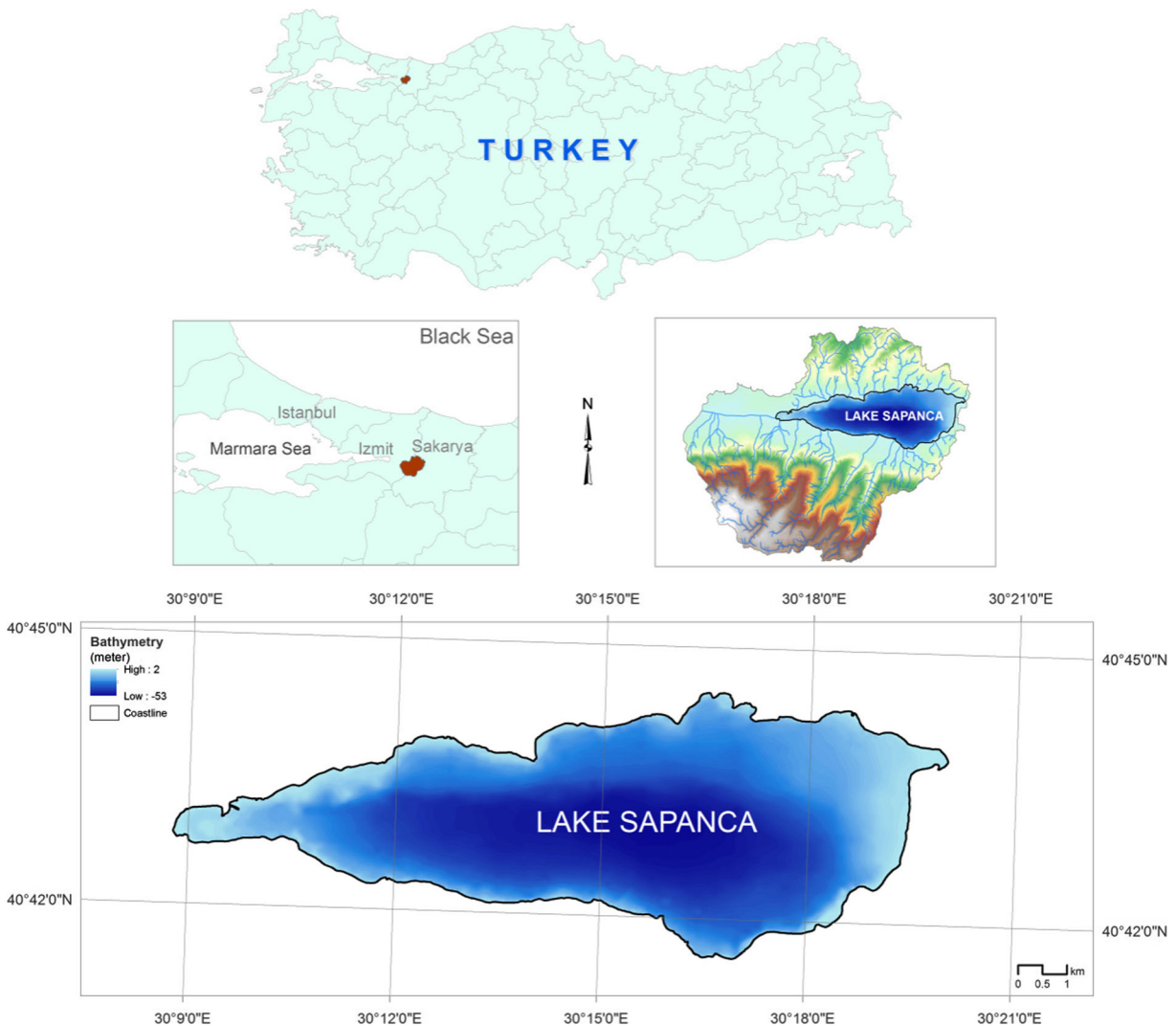


**Fig. 1** Location of the Lake Sapanca (NW Turkey) and its bathymetry

According to DeMartonne, climate classification based on long-term records (1963–2015), the region experiences semi-humid characteristics. The study area lies on tectonic corridor called Sapanca Corridor, mainly consisting of Paleozoic metamorphic rocks (e.g. schist, gneiss, marble) and Mesozoic limestone, marble, and metamorphic rocks. Most of coastal areas have alluvial deposits formed late Pliocene—Quaternary, besides some metamorphic rocky formations along the coast.

The lake reflects the characteristics of oligotrophic clear and warm monomictic lake and it has a surface area of 47 km<sup>2</sup> with a maximum width of ~5 km and length of ~16 km; the average height is 31 m above the sea level (Gurbuz and Gurer 2008). Cark creek in the east is the only outlet draining Lake Sapanca and

empties into the Black Sea. Two large residential areas (Sakarya and Izmit) located in the eastern and western portion of the lake and a rapid rise in population in surrounding areas increase freshwater demand for industrial and domestic purposes. During the drought in 2014, a rapid decrease in water level of Lake Sapanca attracted great attention among the communities settled around the lake (WWF 2015). The lake Sapanca supplies freshwater to the city of Sakarya (~1 million populations), and 90% demand of drinking water is supplied from the lake. Besides, the lake also has been used as a source of freshwater by the surrounding city of Izmit and an industrial institution entitled TUPRAS (Turkish Petroleum Refineries Corporation). The lake is located in the route of the seasonal migration zone for numerous

bird populations (e.g., *Fulica atra*, *Aythya fuligula*, *Oxyura leucocephala*, *Phalacrocorax pygmeus*, *Circus aeruginosus*, *Dendrocopus cyriacus*, *Himantopus himantopus*, *Lxobrychus minutus*). The lake is also a desired environment for terrestrial and aquatic lives (e.g., *Lutra lutra*, *Tinca tinca*, *Aspius aspius*, *Cyprinus carpio*, *Vimba vimba*, *Bombina bombina*, *Thymelicus acteon*) (Doga Society 2006).

## Materials and methods

### Data set

Historical lake shoreline positions were derived from multi-temporal satellite imagery. Six scenes of Landsat 1-5 Multispectral Scanner (MSS), Landsat-7 Enhanced Thematic Mapper Plus (ETM+), and Landsat-8 Operational Land Imager (OLI/TIRS) images were collected from the United States Geological Surveys (USGS), Earth Explorer (<http://www.earthexplorer.usgs.gov>) for a period from 1975 to 2016 (Table 1). A geometrically corrected digital aerial image (10-m resolution) was also collected from a public institution in Sakarya and used as the primary source for geolocating the satellite imagery. All these images are required to be in high quality, relatively cloud free, or free of sensor defects (at least over the shorelines). During that process, imagery acquisition times were taken into consideration (17th June–15th July) in order to minimize the seasonal variation, corresponding to Lake Sapanca's dry session. The 1975 MSS imagery had 80 m spectral resolution with a temporal resolution of 18 days; the 1985 to 2016 Landsat imagery has a spectral resolution of 30 m and a temporal resolution of 16 days. Landsat (MSS) imagery consists of four spectral bands with two visible (VIS) in

green and red wavebands and two near-infrared (NIR) bands. Landsat-7 (ETM+) has band 1–3 of VIS spectrum, band 4 of NIR, band 5–7 of mid-infrared (MIR), band 6 of thermal infrared (TIR), and band 8 of panchromatic. The latest version of Landsat is Landsat-8 Operational Land Imager (OLI/TIRS) which has new infrared spectral bands of 9, 10, and 11.

Other materials collected included meteorological (e.g. precipitation, evaporation) and water level dataset. These were engaged to evaluate hydrologic impacts on shoreline displacements. Mean annual precipitation and evaporation data were obtained from the meteorological station of Sakarya for a period of 54 years. Bathymetric maps of Lake Sapanca were used for computing lake volume, and GPS (Global Position System) in the field was used to collect 30 points along the shoreline for better accuracy during classification.

### Methodology

The basic methodology involved the application of four various steps as follows: (1) pre-processing of images, (2) historical shoreline delineation, (3) shoreline displacement assessment, (4) climate and hydrological analysis (Fig. 2). ERDAS 9.2, DSAS 4.2, and ArcGIS 10.1 computer programs were mainly used for processing the multi-temporal satellite images.

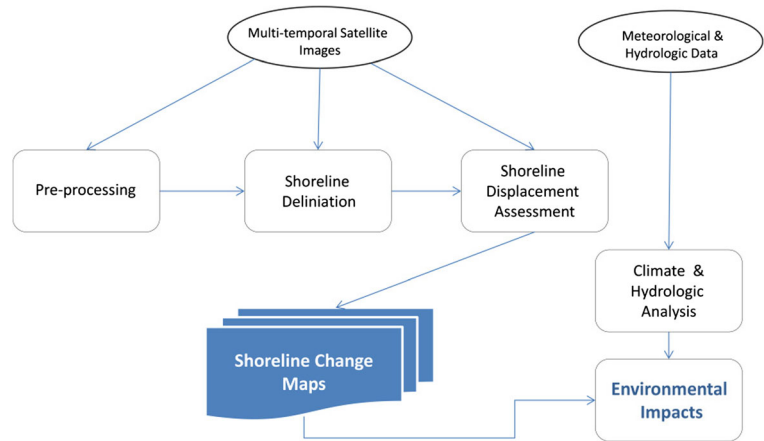
### Pre-processing of images

Pre-processing of satellite images consists of cropping the image for the research area to save storage in the computer and time. The raw images generally contain some degree of defects including geometric distortions, radiometric distortion, and noise cloud effects. To reduce these undesirable errors, radiometric correction

**Table 1** Properties of satellite images and an orthophotograph utilized in the research

Acquisition date	Satellite/sensor	Resolution			
		Spectral (m)	Temporal (day)	Radiometric (bit)	Spectral (band)
17/June/1975	Landsat MSS	80	18	7	4
24/June/1985	Landsat MSS	30	16	8	8
9/July/1995	Landsat ETM+	30	16	8	8
10/July/2014	Landsat (OLI/TIRS)	30	16	12	11
15/July/2016	Landsat (OLI/TIRS)	30	16	12	11
04/June/2011	Areal image (ortho)	10	5	10	12

**Fig. 2** Overall process of coastline change detection



was performed to all Landsat images. Geometric correction is also a fundamental application for historical change detection during pre-processing stage because all images were not geo-rectified with the same degree of accuracy, such as a significant disparity observed in the case of Landsat MSS images. An aerial image (10-m resolution) of 2011 was utilized as a reference map in order to georeference Landsat ETM+ image acquired in 1995 into the Universal Transverse Mercator (UTM 36th Zone North) coordinate system through image-to-image registration. Then Landsat ETM+ image was assigned as a reference map, to which all other Landsat images were georeferenced using image-to-image registration with the root mean square error (RMSE) of ±0.5 pixel. During each georeferencing process, more than 30 well distributed ground control points (GCPs) were collected for better positional accuracy. The polynomial transformation model and the nearest neighbor resampling techniques were applied to all images.

**Shoreline delineation**

Multispectral Landsat imagery is an appropriate dataset for extracting water bodies from lands, so lake water body was extracted by using remote sensing and GIS techniques, which contains several digital image processing and geographic overlay processes. Various methods are currently in use of shoreline delineation from multispectral images (Dellepiane et al. 2004); however, no single method is applicable to various imageries. For example, supervised classification (Sener et al. 2009; Hereher 2011), unsupervised classification (Ekercin 2007), and band ratio (Alesheikh et al. 2007; Karimi and Mobasheri 2011; Sarwar and

Woodroffe 2013); histogram thresholding (Ryu et al. 2002; Cui and Li 2011; Bachofer et al. 2014) were considered appropriate methods for shoreline detection and extraction. Also, band indices Normalized Difference Water Index (NDWI) (Kalkan et al. 2013) and Modified Difference Water Index (MNDWI) have been applied in few literatures (Xu 2006; Nsubuga et al. 2015). In order to extract water information from satellite images, NDWI was initially practiced by McFeeters (1996) to compute water dimensions for wetland environments. Resulting values of NDWI represent that areas covered with water have positive values; however, areas with vegetation or soil tend to have zero or negative values (McFeeters 1996).

$$NDWI = \frac{Band\ 2 - Band\ 4}{Band\ 2 + Band\ 4}$$

Later version of NDWI is called MNDWI generated by Xu (2006). Water features were given in positive values as two classes (water and non-water features).

$$MNDWI = \frac{Band\ 2 - Band\ 5}{Band\ 2 + Band\ 5}$$

In the present study, two water indexes (NDWI and MNDWI) and supervised classification techniques were applied to compare accuracy of the results in shoreline delineation. Based on the results, supervised classification generated more accurate statistics, so this method was applied in the study. During supervised classification, signature editing was utilized to determine the classes as water and non-water surfaces using Gaussian maximum likelihood algorithms for six different satellite images in the image processing software. Then, accuracy assessment with 100 randomly derived from

sample points was carried out through each year, and then compared with the classified image and real data on the ground. The overall accuracy was found more than 87%, which is an acceptable range for the purpose of this research. The final step was the export of six different shorelines into shape file for further processes in ArcGIS 10.1 software.

### Shoreline displacement assessment

The discrete shorelines were delineated from the multi-temporal images in ERDAS 9.2 software, and then all input data were transported into ArcGIS 10.1 software. The rate of historical shoreline displacements along Lake Sapanca was computed using the Digital Shoreline Analysis System (DSAS 4.2) extension that enhances the functionality of ArcGIS software, developed by the United States Geological Surveys (USGS) (Thieler et al. 2009). The DSAS leads a researcher through the major steps of historical shoreline displacement analysis by allowing them to compute rate of shoreline displacement from multi-temporal satellite images. The extension consists of three main steps that define a baseline, generating orthogonal transects along coastline and compute rates of change by using the least median of squares (LMS), end point rate (EPR), linear regression rate (LRR), and weighted linear regression (WLR). Shoreline change rates were calculated for each transect, including LMS, EPR, LRR, and WLR of change.

An analysis of short-term shoreline changes for shorter periods of 11 years (2005–2016) and long-term variation (1975–2014; 1975–2016) was performed in the study. The baseline was manually generated onshore about 100 m landward, respecting to be parallel to the dominant tendency of six different shorelines. In order to cover the region of major shoreline displacements, transects were set to be at 150 m spacing alongshore, which means the rates were calculated every 150 m along the entire lake. A total number of 343 transects were automatically generated, and statistics were extracted for a 90% confidence interval. For the purpose of detailed analysis—in shoreline displacement rates, the coast of Lake Sapanca was subdivided into four analysis regions as Reg-1, Reg-2, Reg-3, and Reg-4. These regions were defined based on the coast where higher magnitude of shoreline change was experienced in the past decades. The Reg-1 is 5 km long starting from eastern Kartepe; Reg-2 with the length of 3.5 km extends along the southern portion of Esme; Reg-3 with the length of 5 km long stating from Beskopru to Arifbey; the Reg-4 is a 3.5-km-long section along the coastline of the city of Sapanca (Fig. 3).

### Climate and hydrology:

Hydrologic input to Lake Sapanca is controlled by 18 creeks (15 million m<sup>3</sup>/year), rainfall (34 million m<sup>3</sup>/year), and groundwater (15 million m<sup>3</sup>/year), and the water is primarily lost from the lake through industrial/

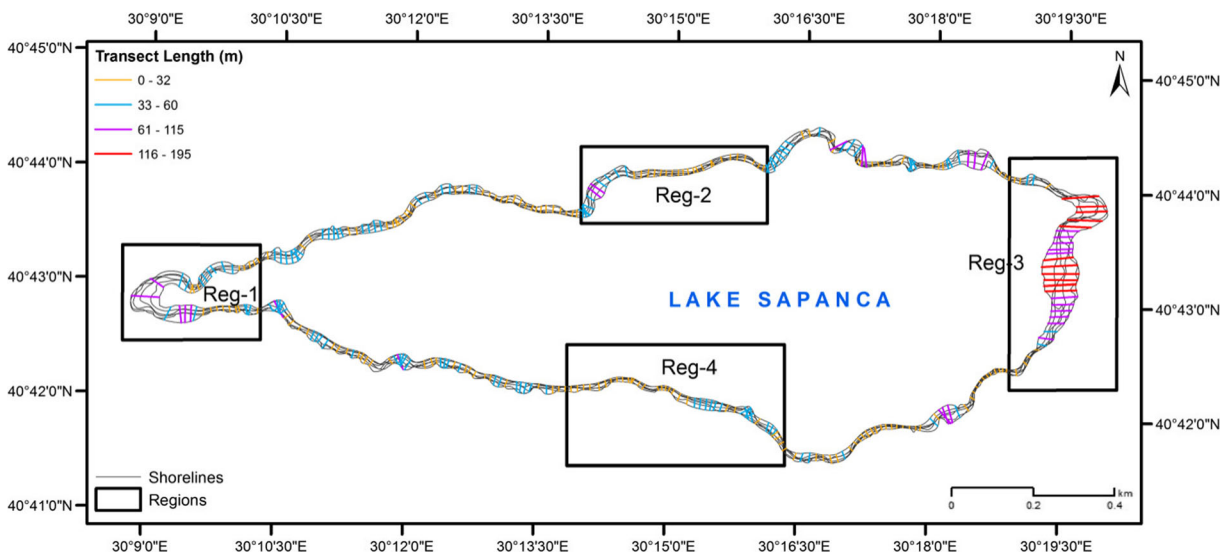


**Fig. 3** Interpretation of four broad regional sectors along the shoreline of Lake Sapanca

domestic purposes (120 million m<sup>3</sup>/year), Cark Creek (56 million m<sup>3</sup>/year) and evaporation (24 million m<sup>3</sup>/year) (WWF 2015). Thus, the change of the lake mainly reflects a combination of climate parameters, creek discharge, or anthropogenic usage. In the present research, broad climate and hydrological data assessments have been made to determine effects of climate change and human alteration on Lake Sapanca. In order to determine long-term trends for rainfall and surface water level, the Mann-Kendall test results were used as a reference. Additionally, previous studies have been searched; bathymetry and long-term water level data were utilized to determine the most dominant factors controlling shoreline displacements in the region.

**Results**

Along Lake Sapanca coastline, four broadly subdivided regions (Reg-1, Reg2, Reg-3, Reg-4) were generated to investigate space and time variability in shoreline changes. The historical shoreline lengths and change rates were computed and analyzed by using DSAS for the years of 1975, 1985, 1995, 2005, 2014, and 2016. Results furthermore indicated that the magnitudes of shoreline change rates calculated from multi-temporal images are distinctly different based on the rate calculation method. The statistics represent accretion as positive values and erosion as negative values. The average rate of long-term shoreline displacement for the entire coast was computed as 2.7 m/year of progradation with an uncertainty of 0.2 m/year at a 90% confidence interval. This rate was based on 343 individual transects, of which 99% was determined to be accumulated. The maximum rates of accretion and erosion were calculated as 11.9 m/year and -0.6 m/year ±0.2 m/year, respectively. None of the coast had erosion rates greater than -0.7 m/year (90% confidence interval). That should be noted that a higher rate of erosion has been mainly experienced along the northwest portion of the lake (in Reg-3). The accretion was also observed at the Reg-3 along the cost of Arifiye and Reg-1 along the cost of Kartepe, and also, deltaic formations had some degree of gradual sediment accumulation, in general. Table 2 shows the rates of the shoreline changes in four locations along the lake’s shore. The LMS, EPR, LRR, and WLR exhibited the higher shoreline position changes within Reg-1 and Reg-3. In recent years, the magnitude

**Table 2** Statistics of Sapanca shoreline in different segments from 1975 to 2016 (m/year)

Segments	Statistical characters	90% confidence interval			
		LMS	EPR	LRR	WLR
REG-1	Max	7.2	7.1	10.2	13.3
	Min	1.1	0.5	0.02	0.7
	Mean	2.6	2.2	2.8	3.5
REG-2	Max	4.3	3.9	4.0	6.7
	Min	0.5	0.8	0.7	1.3
	Mean	2.1	2.4	2.1	2.9
REG-3	Max	18.3	11.9	14.7	17.5
	Min	0.6	-0.6	0.3	1.5
	Mean	5.3	5.0	7.1	8.0
REG-4	Max	5.1	5.0	5.5	7.1
	Min	0.04	-0.1	0.2	1.4
	Mean	2.2	2.4	2.4	3.4

of water level change reflected more frequent and distinct variations for the entire coast of Lake Sapanca.

Shoreline displacements along the Reg-1

The average rate of shoreline position changes between 1975 and 2016 along the coastline of Reg-1 is shown in Fig. 4. Although the shoreline positions were observed to be consistent during 1975 and 1985, the shoreline positions began to fluctuate along the western portion of Reg-1 after the year of 1985 as a result of initiation of lower rainfall mean as well as higher variability. However, more aggressive fluctuations have been seen in the bay since 2005 due to accretion, climate change, and anthropogenic influences. The average rate of shoreline change was 2.2 of progradation with an uncertainty of 0.4 m/year. The maximum shoreline accretion rate was found 7.1 ± 0.4 m/year in Reg-1. From 1985 to 2014, the maximum shoreline headway for the coast of Reg-1 was mainly resulted from an excessive drought between 2013 and 2014 and increased demand on freshwater drained from the lake after the year of 2013. Between 2014 and 2016, the shoreline of the lake was moved to the west due to a significant rise in rainfall, which has been observed since late 2014. As shown in Fig. 4, shoreline changes multivariate in recent years. One of the highest changes in bay shoreline position was observed at this region because shallow water area is wider on the western portion of the lake.

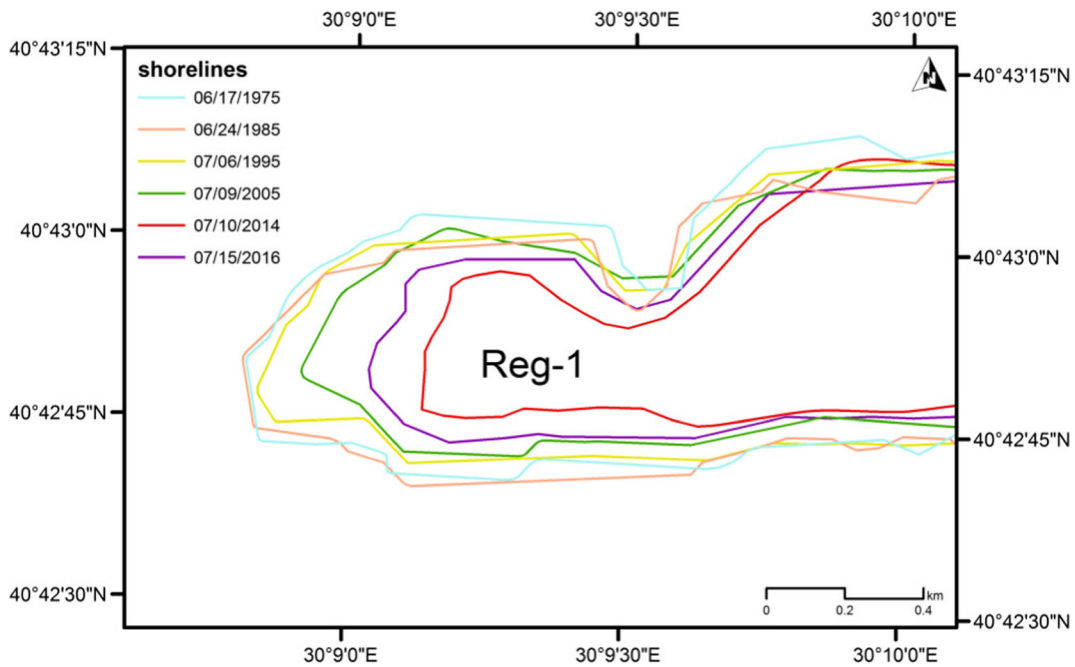


**Fig. 4** Multi-temporal shoreline positions of the Reg-1

**Shoreline displacements along the Reg-2**

The change of shoreline positions were observed to be consistent between 1975 and 2016 along Reg-2; however, deltaic formations formed by surrounding creeks (e.g. Yukaridere, Asagiderekoy, Esme) show higher differentiation due to sediment accretion through the years (Fig. 5). The rate of accretion is more dominant than the rate of erosion due to continuous supply from nearby rivers along the Reg-2. Though shoreline exhibited

stability in general, the deltaic formations of Esme and Asagidere experienced the highest shoreline displacements within the region. Sediment accumulation plays a significant role in the positional changes of shorelines at this coast. This accretion resulted from an excessive deposition of sediment transported by Esme and Asagiderekoy creeks. The average shoreline change rate was calculated 2.4 m/year of progradation with an uncertainty of 0.2 m/year. More specifically, a slower accretion was shown at the central portion of Reg-2

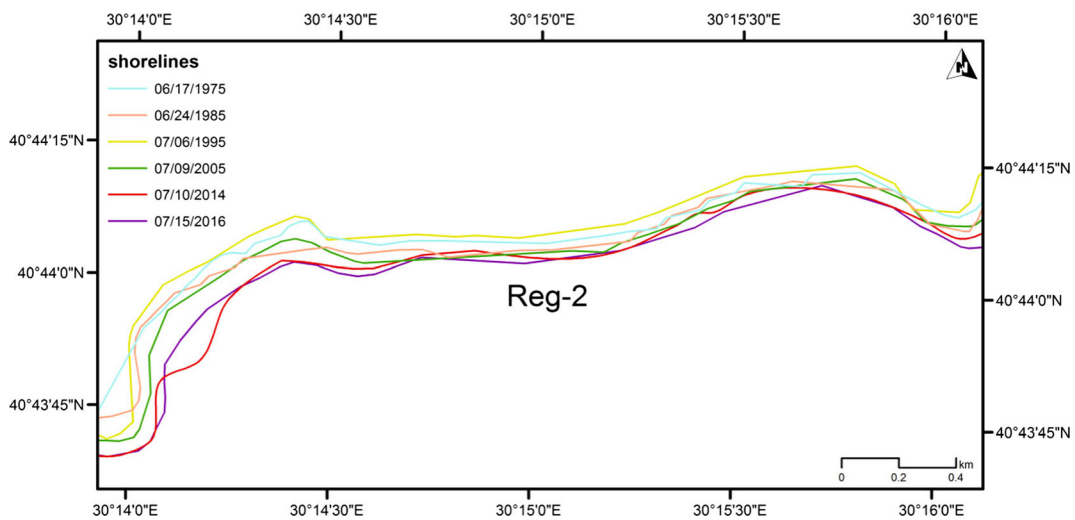


**Fig. 5** Multi-temporal shoreline positions of the Reg-2



when compared with accumulation on deltas with an average rate of  $3.9 \pm 0.2$  m/year. The shoreline position displayed stability at the center of Reg-2 because of the blockage of eastward groin constructed for motorway (D100) along the central part of Reg-2.

Shoreline displacements along the Reg-3

The 41 years of shoreline change rates along the Reg-3 segment is displayed in Fig. 6. The figure shows a consistency in shoreline position between 1975 and 1985. The shoreline position of 1995 and 2005 also remained unchanged in this section; however, they more aggressively started to differentiate after the years of 2005. The shoreline position was displaced toward the west side from 1985 to 2014, but the north and south coastline exhibited stability. Moreover, the average shoreline advancement was calculated 5.0 with an

uncertainty level of 1 m/year. For the entire cost of Lake Sapanca, the maximum accretion and erosion rates of 11.9 and  $-0.62 \pm 1$  m/year were computed in this region. The displacements in shorelines after the year of 2005 mainly resulted from an extensive drought that took place during 2013 and 2014 and an increase in freshwater usage after the year of 2013. Afterward, western shoreline was extensively moved to the east after the year of 2014 because of a significant rise in rainfall events. The shore is quite sensitive to displacements in this section as a result of wider shallow water area on the east coast of the lake, and also sediment deposition extensively occurred under the sedges along the eastern coast. As shown in Fig. 6, shoreline changes were highly variable in recent years due to changes in water level caused by natural (e.g. rainfall variation, waves, and winds) and anthropogenic influences (e.g. over usage of water, developmental projects) in recent decades.

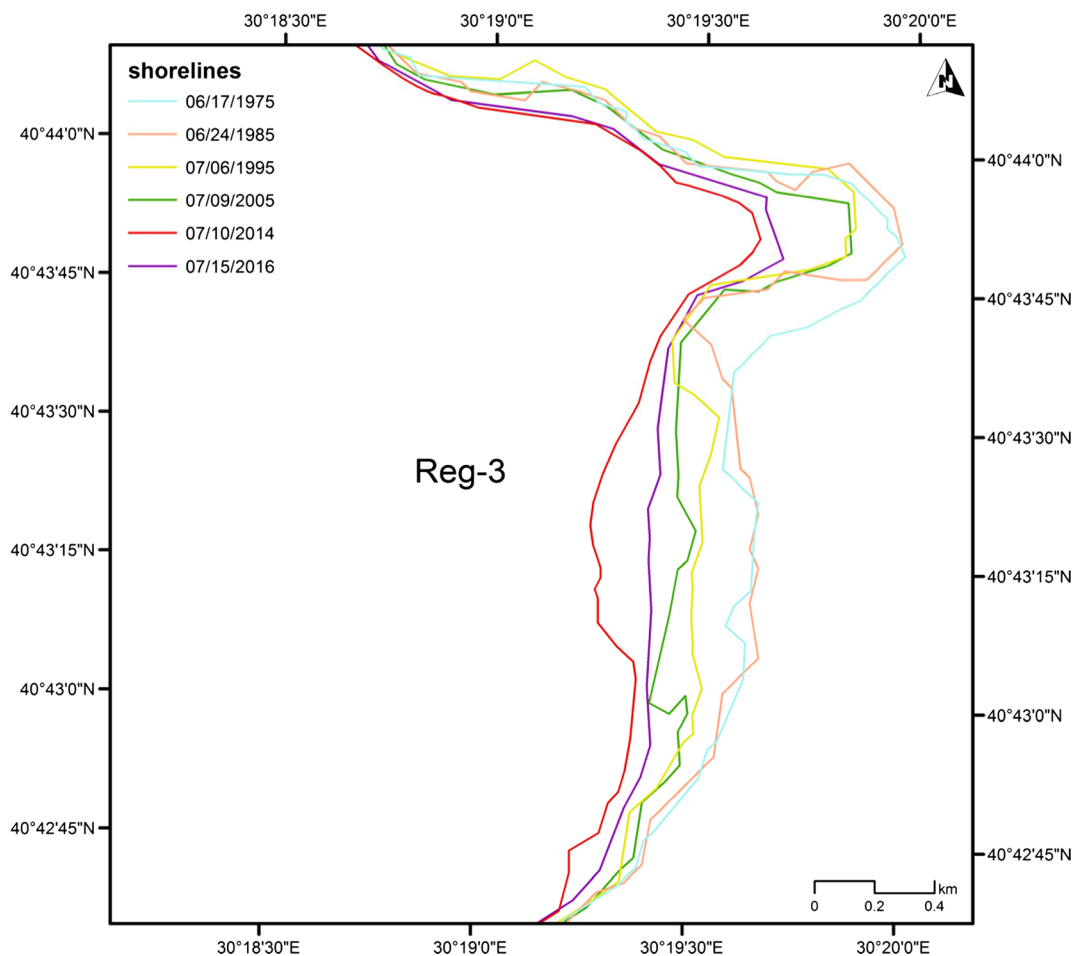
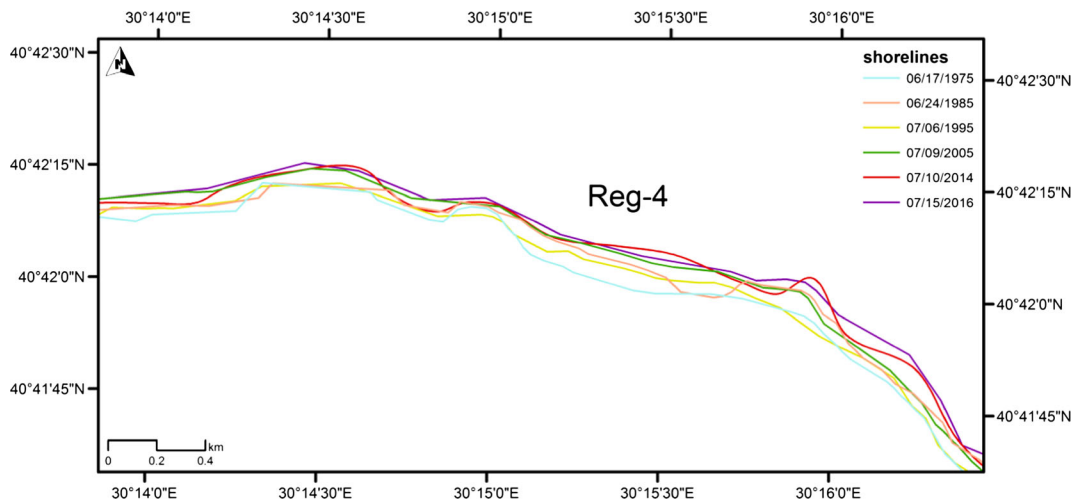


Fig. 6 Multi-temporal shoreline positions of the Reg-3



**Fig. 7** Multi-temporal shoreline positions of the Reg-4

Shoreline displacements along the Reg-4

During monitoring historical shoreline displacements along the coast of Sapanca district (Reg-4 sector), coastline exhibited stability in general (Fig. 7). The reason why shoreline position displayed stability may be resulted from a groin constructed for the purpose of stabilizing shore to avoid the damages to lakeside parks in the district of Sapanca. Additionally, packaged drinking water usage have reduced river flow and sediment supply from Istanbul and Mahmudiye creeks. The shorelines from the years of 2005, 2014, and 2016 resembled each other and laid straighter forward when comparing these positions with earlier years. The position of shore

has also been gradually moved northward by the center of Reg-4 since 1975 due to the fact that sediment deposition more extensively took place than erosion along the coast. This was mainly resulted from a continuous sediment input via Mahmudiye and Istanbul Creeks along the shore. The average shoreline advancement was 2.4 m/year with an uncertainty level of 0.4 m/year. A maximum accretion value of  $5.0 \pm 0.4$  m/year was found around the deltaic formation of Mahmudiye and Istanbul creeks. From 1975 to 2016, the lowest rate of shoreline displacement were experienced within Reg-4, which may also be resulted in newly formed delta lobe of the creeks initiated to be washed away by the water; correspondingly, the shore was migrated landward.

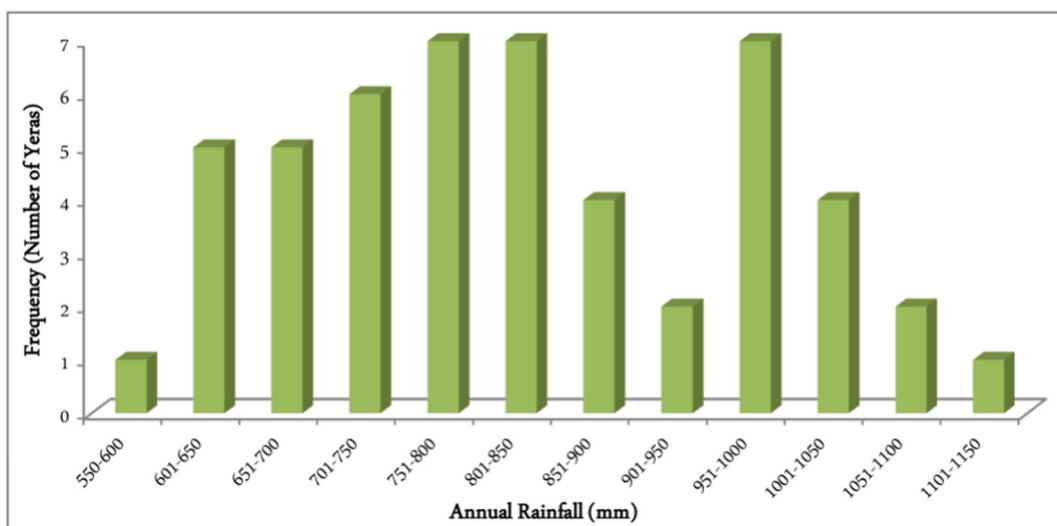


**Fig. 8** Frequency histogram of annual rainfall at Sakarya (1962–2015)

Climate and hydrological analysis

Rainfall is the main source of water for 18 creeks that pour into the lake, and it is one of the most dominant agents that control erosion, accretion, and shoreline change within the lake. The main hydrology of the lake is also controlled by these small creeks over shorter and longer timescales. Therefore, rainfall is one of the most significant variables that must be taken into consideration when analyzing shoreline displacements and water level changes because the changes in water level may also lead to coastal erosion, accretion, and, correspondingly, shoreline displacement. The coefficient of variation (*Cv*) was computed 17% for long-term rainfall data. As illustrated in Fig. 8, rainfall mainly occurs about 780 mm/year.

Lake Sapanca water level had shown a consistency until 2013; however, an extreme drought event took place between 2013 and 2014. The drought which started late spring 2013 to late summer 2014 resulted in a significant drop in the length, area, and volume to 35.1 km, 40.3 km<sup>2</sup>, and 1157 m<sup>3</sup>, respectively (Table 3). This extreme event rapidly dropped the level of water from 31.6 m, which is 60 years mean annual water level, about 2 m in the year of 2014. In terms of trend in precipitation, a decreasing trend has been seen in the study area. Ceribasi and Dogan (2016) applied the Mann-Kendall test to determine long-term trend in precipitation, and they concluded a significant decrease in rainfall with a negative trend ( $Z = -3.29$ ) in the region. Besides drought, an increase in draining freshwater from the Lake Sapanca after 2013 caused loss of water (WWF 2015), which altered the lake’s shoreline in the recent

**Table 3** Historical measurement of the shoreline length, surface area, and volume of Lake Sapanca

Years	Length (km)	Area (km <sup>2</sup> )	Volume (m <sup>3</sup> )
1975	39.9	45.7	1348
1985	38.7	45.3	1279
1995	38.1	45.1	1252
2005	37.3	43.3	1221
2014	35.1	40.3	1157
2016	36.0	41.6	1203

years. However, rise in rainfall event in the year of 2015 and 2016 contributed to overcome the loss of water into the lake. Figure 9 illustrates a temporal variation in water level and rainfall, representing rainfall and lake water level, has similar drops and rises through years.

In the present study, the Mann-Kendall test was applied to determine long-term trend in surface water level due to the lack of long-term river discharge data from the creeks, which control the main hydrology of the lake. The results of the Mann-Kendall test for water level, *p* value ( $p < 0.05$ ) and Kendall’s tau found as 0.0001 and  $-0.16$ , respectively. The main apparent element of the result is that statistically significant downward trend was seen in both rainfall and water level as a result of combination of natural and anthropogenic influences in the region. Recently, Sapanca coast faces higher magnitude of fluctuations caused by natural phenomena (e.g. climate change, winds) and human alterations such as developmental projects, overuse of water for residential and industrial purposes along the coast, and packaged drinking water factories located along the creeks, which reduces annual discharge rate into the lake.

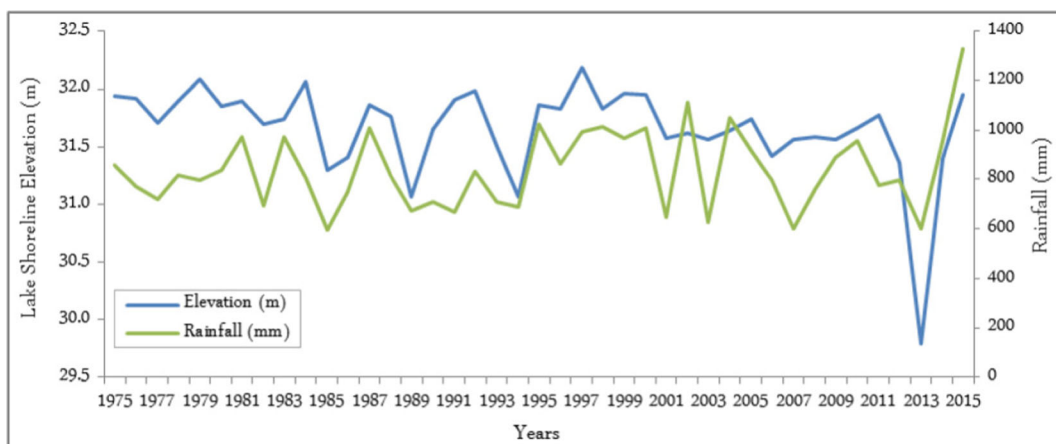


**Fig. 9** Long-term monthly water level (m) and rainfall variation (1975–2015)

## Environmental impacts of shoreline displacements

Lake shorelines provide a transitional habitat for both terrestrial and aquatic organisms, and they produce a diverse biota and fauna comparing to the pelagic water (Schmieder 2004). A diversity of microorganisms, microinvertebrates, and algae in the littoral zone attracts biotic and abiotic species due to providing rich food resources, spawning sites, etc. Therefore, a considerable part of primary production for birds, fishes, macroinvertebrates, and flora takes place in shallow water areas. In addition, nutrients in fertilizers, sediment, and sewage effluents are likely to be interspersed by nearshore algae when they entered into the lake. Due to very specific habitat requirements of shoreline organisms, water level fluctuation may cause loss of some intolerant species, accordingly expanding the area of barelands. Under extensive water level fluctuation with especially higher annual variation, most littoral organisms tend to have lower change of survival (Smith et al. 1987).

Although extreme water level fluctuations disturb littoral organisms, moderate water level fluctuations may have positive effects on biodiversity in littoral zones. For instance, water level shows a decreasing trend over 41 years, so some species including sedges expanded in wetland areas of Lake Sapanca (especially in the Reg-1 and Reg-3). These sedges provide a desired habitat (e.g. canopy/shade, hiding place, nutrient) for wildlife. As mentioned above, the average shoreline fluctuation rate was 5.0 with an uncertainty level of 1 m/year in Reg-3 (Table 4), which is acceded as extreme fluctuation threshold by Smith et al. (1987). The study reveals that an area with average fluctuation rate is greater than 5–7 m tend to have a significant degradation on its biota and fauna.

**Table 4** Rate of shoreline accretion along the shore of Lake Sapanca

Segments	Number of transects	EPR	Uncertainties 90% confidence	Remarks
REG-1	30	2.2	0.4	Moderate accretion
REG-2	45	2.4	0.2	Moderate accretion
REG-3	35	5	1.0	High accretion
REG-4	35	2.4	0.4	Moderate accretion

## Conclusion

The present study on shoreline changes confirms that multi-temporal Landsat images with the integration of GIS technology coupled with DSAS has been a very useful tool for historical shoreline change assessments along Lake Sapanca coastline. This method is capable of providing a comprehensive aspect regarding natural and anthropogenic influences on spatiotemporal changes in shoreline position, as well as the pattern of accretion and erosion along coastal areas. The regions of Reg-1 and Reg-3 with shallow water cost have been subjected to significant changes in the last four decades (1975–2016). The average rate of long-term shoreline displacement for the entire cost was computed as 2.7 m/year of progradation with an uncertainty of 0.2 m/year. The maximum rates of accretion and erosion were calculated as 11.9 and –0.6 m/year, respectively. The main causes of changes along these shores are mainly related to the natural shifting in rainfall intensity and anthropogenic effects including developmental projects and overuse of freshwater drained from the lake in the last decades.

Although westerly and easterly coasts of the lake reflect more frequent and distinct changes, some part of the coast remained stable. Indeed, deltaic formations of relatively larger creeks along the coast have experienced significant shoreline changes in Reg-2 and Reg-4. The maximum shoreline advancements along the deltaic coast of Esme, Asagidere, Mahmudiye, and Istanbul creeks ranged from 3.9 to 5.0 m/year. An excessive deposition of sediment transported by the creeks plays a more important role in coastline position changes at deltas. Additionally, the groins constructed for the purpose of stabilizing shore to avoid damages to residential facilities and washing away newly formed delta lobes resulted to more stable shore in the district of Sapanca. It should be noted that the magnitude of water level change reflected more frequent and distinct variations in recent years, so interdisciplinary coastal management plans should be made for further shoreline displacements along the coast. Without appropriate precautions, severe fluctuation in shoreline of Lake Sapanca will cause environmental and economic consequences, especially in the coasts where fluctuation occurred more frequently. Recycling waste water for industrial usage, fining out new resources, and primarily drawing water from more temperate locations should be performed in order to reduce fluctuation rate, correspondingly conserving coastal zone of the lake.

## References

- Al Fugura, A., Billa, L., & Pradhan, B. (2011). Semi-automated procedures for shoreline extraction using single RADARSAT-1 SAR image. *Estuarine, Coastal and Shelf Science*, 95(4), 395–400.
- Alesheikh, A. A., Ghorbanali, A., & Nouri, N. (2007). Coastline change detection using remote sensing. *International journal of Environmental Science and Technology*, 4(1), 61–66.
- Al-Hatrushi, S. M. (2013). Monitoring of the shoreline change using remote sensing and GIS: a case study of Al Hawasnah tidal inlet, Al Batinah coast, Sultanate of Oman. *Arabian Journal of Geosciences*. doi:10.1007/s12517-011-0424-2.
- Bachofer, F., Queneherve, G., & Marker, M. (2014). The delineation of paleo-shorelines in the Lake Manyara Basin using TerraSAR-X data. *Remote Sensing*. doi:10.3390/rs6032195.
- Bayram, B., Seker, D. Z., Acar, U., Yuksel, Y., Anil, H., Ari, G., & Cetin, I. (2013). An integrated approach to temporal monitoring of the shoreline and basin of Terkos Lake. *Journal of Coastal Research*, 29(6), 1427–1435.
- Bin, O., Kruse, J. B., & Landry, C. E. (2008). Flood hazards, insurance rates, and amenities: evidence from the coastal housing market. *Journal of Risk and Insurance*, 75(1), 63–82.
- Boahen, K. A., Emmanuel, A. M., Kwaku, K. K., & Osman, A. (2014). Socio-economic impact of Lake Bosomtwe shoreline changes on catchment residents in Ghana. *International Journal of Scientific and Research Publications*, 4(2), 1–7.
- Bumshick, S., & Kyuhan, K. (2015). Estimation of shoreline change using high resolution images. *Procedia Engineering*, 116, 994–1001.
- Ceribasi, G., & Dogan, E. (2016). Trend analysis of average annual for Black Sea and Sakarya Basins. *SDU International Journal of Technological Science*, 7(1), 1–7.
- Coops, H., Beklioglu, M., & Crisman, T. L. (2003). The role of water-level fluctuations in shallow lake ecosystems—workshop conclusions. *Hydrobiologia*, 23(27), 506–509.
- Cui, B. L., & Li, X. Y. (2011). Coastline change of the Yellow River estuary and its response to the sediment and runoff (1976–2005). *Geomorphology*, 127, 32–40.
- Dellepiane, S., DeLaurentiis, R., & Giordano, F. (2004). Coastline extraction from SAR images and a method for the evaluation of the coastline precision. *Pattern Recognition Letters*, 25, 1461–1470.
- Doğa Society. (2006). *Important nature fields of Turkey*. Turkey: Ankara.
- Durduran, S. S. (2010). Coastline change assessment on water reservoirs located in the Konya Basin Area, Turkey, using multitemporal Landsat imagery. *Environmental Monitoring & Assessment*, 164, 453–461.
- Ekercin, S. (2007). Coastline change assessment at the Aegean Sea coasts in Turkey using multitemporal Landsat Imagery. *Journal of Coastal Research*, 23(3), 691–698.
- El-Asmar, H. M., & Hereher, M. (2011). Change detection of the coastal zone east of the Nile Delta using remote sensing. *Environmental Earth Sciences*, 62(4), 769–777.
- Ford, M. (2013). Shoreline changes interpreted from multi-temporal aerial photographs and high resolution satellite images: Wotje Atoll Marshall Islands. *Remote Sensing of Environment*, 135, 130–140.
- Gurbuz, A., & Gurer, O. F. (2008). Anthropogenic affects on lake sedimentation process: a case study from Lake Sapanca, NW Turkey. *Environmental Geology*. doi:10.1007/s00254-007-1165-0.
- Hereher, M. (2011). Mapping coastal erosion at the Nile Delta western promontory using Landsat imagery. *Environmental Earth Sciences*, 64(4), 1117–1125.
- Jangir, B., Satyanarayana, A. N. V., Swati, S., Jayaram, C., Chowdary, V. M., & Dadhwal, V. K. (2016). Delineation of spatio-temporal changes of shoreline and geomorphological features of Odisha coast of India using remote sensing and GIS techniques. *Natural Hazards*. doi:10.1007/s11069-016-2252-x.
- Kalkan, K., Bayram, B., Maktav, D., & Sunar, F. (2013). Comparison of support vector machine and object based classification methods for coastline detection. *International Archives of the Photogrammetry, Remote Sensing and Spatial Information Sciences*, Volume XL-7/W2, ISPRS2013-SSG, Antalya, Turkey.
- Karimi, N., & Mobasheri, M.R. (2011). Shoreline change analysis of Urmia Lake using multi-temporal satellite images. Eighteenth National Conference on Geomatics, Iran, Tehran. 88–96 p.
- Kuleli, T. (2010). Quantitative analysis of shoreline Changes at the Mediterranean Coast in Turkey. *Environmental Monitoring & Assessment*, 167(4), 387–397.
- Kumari, P., Jnaneswari, K., Rao, D., & Sridhar, D. (2012). Application of remote sensing and geographical information system techniques on geomorphological mapping of coastal part of East Godavari district. Andhra Pradesh, India. *International Journal of Engineering Science Technology*, 4, 4296–4300.
- Lewin, W. C., Mehner, T., Ritterbusch, D., & Bramick, U. (2014). The influence of anthropogenic shoreline changes on the littoral abundance of fish species in German lowland lakes varying in depth as determined by boosted regression trees. *Hydrobiologia*. doi:10.1007/s10750-013-1746-8.
- Liu, H., Sherman, D., & Gu, S. (2007). Automated extraction of shorelines from airborne light detection and ranging data and accuracy assessment based on Monte Carlo simulation. *Journal of Coastal Research*, 23(6), 1359–1369.
- Mann, T., Bayliss, T. S., & Westphal, H. (2016). A geomorphic interpretation of shoreline change rates on Reef Islands. *Journal of Coastal Research*, 32(3), 500–507.
- Martin, P. H., LeBoeuf, E. J., Dobbins, J. P., Daniel, E. B., & Abkowitz, M. D. (2005). Interfacing GIS with water resource models: a state-of-the-art review. *Journal of the American Water Resources Association (JAWRA)*. doi:10.1111/j.1752-1688.2005.tb03813.x.
- McFeeters, S. K. (1996). The use of Normalized Difference Water Index (NDWI) in the delineation of open water features. *International Journal of Remote Sensing*, 17(7), 1425–1432.
- Moussa, M., Baccar, L., & Ben Khemis, R. (2005). La lagune de Ghar El Melh: Diagnostic écologique et perspectives d'aménagement hydraulique. *Revue des Sciences Del'Eau*, 18, 13–26.
- Mujabar, P. S., & Chandrasekar, N. (2013). Shoreline change analysis along the coast between Kanyakumari and Tuticorin of India using remote sensing and GIS. *Arabian Journal of Geosciences*, 6(3), 647–664.

- Nandi, S., Ghosh, M., Kundu, A., Dipanwita, D., & Moumita, B. (2016). Shoreline shifting and its prediction using remote sensing and GIS techniques: a case study of Sagar Island, West Bengal (India). *Journal of Coastal Conservation*. doi:10.1007/s11852-015-0418-4.
- Natesan, U., Thulasiraman, N., Deepthi, K., & Kathiravan, K. (2013). Shoreline change analysis of Vedaranyam coast, Tamil Nadu, India. *Environmental Monitoring & Assessment*, 185(6), 5099–5109.
- Nsubuga, F. N., Botai, J. O., Olwoch, J. M., Dew Rautenbach, C. J., Kalumba, A. M., Tsela, P., et al. (2015). Detecting changes in surface water area of Lake Kyoga sub-basin using remotely sensed imagery in a changing climate. *Theoretical and Applied Climatology*. doi:10.1007/s00704-015-1637.
- Ormeçi, C., & Ekerçin, S. (2007). An assessment of water reserve change in the Salt Lake, Turkey through multitemporal Landsat imagery and real-time ground surveys. *Hydrological Processes*. doi:10.1002/hyp.6355.
- Paterson, S.K., O'Donnell, A., Loomis, D.K., & Hom, P. (2010). The social and economic effects of shoreline change: North Atlantic, South Atlantic, Gulf of Mexico, and Great Lakes regional overview. Final Report, Human Dimensions of Natural Resource Management Research Unit, Department of Natural Resources Conservation University of Massachusetts, Amherst, MA.
- Ryu, J. H., Won, J. S., & Min, K. D. (2002). Waterline extraction from Landsat TM data in a tidal flat: a case study in Gosmo Bay, Korea. *Remote Sensing of the Environment*. doi:10.1016/S0034-4257(02)00059-7.
- Sarp, G., & Ozcelik, M. (2016). Water body extraction and change detection using time series: a case study of Lake Burdur, Turkey. *Journal of Taibah Univverity of Science*. doi:10.1016/j.jtusci.2016.04.005.
- Sarwar, M., & Woodroffe, C. D. (2013). Rates of shoreline change along the coast of Bangladesh. *Journal of Coastal Conservation*, 17(3), 515–526.
- Schindler, D. E., & Scheuerell, M. D. (2002). Habitat coupling in lake ecosystems. *Oikos*, 97, 177–189.
- Schmieder, K. (2004). European lake shores in danger—concepts for a sustainable development. *Limnologica*, 34, 3–14.
- Sener, E., Davraz, A., & Sener, S. (2009). Investigation of Akşehir and Eber Lakes (SW Turkey) coastline change with multitemporal satellite images. *Water Resource Management*, 26(4), 727–745.
- Smith, R.V., Belknap, D.F. & Kelley, J.T. (1987). The role of bluff erosion and sediment recycling in shaping Maine's coastline. Geological Society of America Abstract with Programs, 19, 58 p.
- Stockdon, H. F., Sallenger, A. H., List, J. H., & Holman, R. A. (2002). Estimation of shoreline position and change using airborne topographic LiDAR data. *Journal of Coastal Research*, 18(3), 502–513.
- Sudha Rani, N. N. V., Satyanarayana, A. N. V., & Bhaskaran, P. K. (2015). Coastal vulnerability assessment studies over India: a review. *Natural Hazards*. doi:10.1007/s11069-015-1597-x.
- Tagil, S. (2007). Quantifying the change detection of the Uluabat wetland, Turkey, by use of Landsat Images. *Ekoloji*, 16(64), 9–20.
- Tao, S., Fang, J., Zhao, X., Zhao, S., Shen, H., Hu, H., & Turner, B. L. (2015). Rapid loss of lakes on the Mongolian Plateau. *Proceedings of the National Academy of Sciences of the United States of America*. doi:10.1073/pnas.1411748112.
- Temiz, F., & Durduran, S. (2016). Monitoring coastline change using remote sensing and GIS technology: a case study of Acıgöl Lake, Turkey. *IOP Conf. Series: Earth and Environmental Science*. doi:10.1088/1755-1315/44/1/011001.
- Thieler, E.R., Himmelstoss, E.A., Zichichi, J.L., & Ergul, A. (2009). Digital Shoreline Analysis System (DSAS) version 4.0—an ArcGIS extension for calculating shoreline change: U.S. Geological Survey Open-File Report 2008–1278.
- Tonisso, H., Suursarr, U., & Kont, A. (2012). Maps, aerial photographs, orthophotos and GPS data as a source of information to determine shoreline changes, coastal geomorphic processes and their relation to hydrodynamic conditions on Osmussa island, The Baltic sea. *IGRSS*, 12, 987–1159.
- Wallick, J. R., Lancaster, S. T., & Bolte, J. P. (2006). Determination of bank erodibility for natural and anthropogenic bank materials using a model of lateral migration and observed erosion along the Willamette River, Oregon, USA. *River Research & Applications*, 22, 631–649.
- Wang, Y., & Allen, T. R. (2008). Estuarine shoreline change detection using Japanese ALOSPALSAR HH and JERS-1 L-HH SAR data in the Albemarle-Pamlico Sounds, North Carolina, USA. *International Journal of Remote Sensing*, 29, 4429–4442.
- WWF. (2015). *Water risk and economy in Lake Sapanca report*. Istanbul: Gorsel Design and Offset Press.
- Xu, H. (2006). Modification of normalized difference water index (NDWI) to enhance open water features in remotely sensed imagery. *International Journal of Remote Sensing*, 27(14), 3025–3033.
- Yoon, J. H., Kang, S. J., & Oh, T. K. (2008). *Roseovarius aestuarii* sp. nov., isolated from a tidal flat of the Yellow Sea in Korea. *International Journal of Systematic and Evolutionary Microbiology*, 58, 1198–1202.
- Zhang, A., Hu, S., Jin, X., & Sun, W. (2005). A method of merging aerial images and ground laser scans. In: Geoscience and remote sensing symposium. IGARSS '05, 222–225 p.